Interaction of surface states with rows of adsorbed atoms and other one-dimensional scatterers

G. Hörmandinger and J. B. Pendry
Department of Physics, Imperial College, Prince Consort Road, London SW7 2BZ, United Kingdom
(Received 23 August 1994)

This paper investigates the interaction of a surface state with a one-dimensional scattering object on the surface of a metal. Examples are straight rows of regularly spaced adsorbed atoms, and straight step edges. The layer–Korringa-Kohn-Rostoker method is employed to investigate the electronic structure of periodic arrays of rows of adatoms on the Cu(111) surface in a 6×2 geometry, as well as periodic arrays of missing rows to simulate step edges. From these band structures, the behavior of one individual scatterer is extracted by means of a one-dimensional model. Thus we obtain the rates of reflection, transmission, and scattering into the substrate. Rows of adsorbed Cu, Fe, S, and C are considered as well as single and double missing rows. It is found that none of these scatterers comes close to total reflectivity (R=1). Most cases lead to R around 0.3–0.4. The rest of the incoming electrons are mainly transmitted into the surface state on the other side, if the scatterer is a row of Cu or Fe atoms, while they are mainly scattered into the bulk by S and C. The behavior of missing rows is found to lie in between. By counting the number of outgoing states that a surface state can scatter into, qualitative information is obtained for two important situations. First, it is shown that for less than close-packed rows of adsorbed atoms, the ratio of the scattering rate into the bulk to that into the surface state is enhanced because of Bragg scattering. On Cu(111), this enhancement starts at an adatom spacing of $M \geq 2$. Second, it is argued that replacing the semi-infinite substrate by a thin film is unlikely to reduce the loss of electrons into the bulk. While it is found that surface states interact strongly with most adsorbates, our results suggest that the total confinement of surface states within artificially made structures may not be feasible.

I. INTRODUCTION

Surface states have been studied for quite a long time, using photoemission and inverse photoemission spectroscopy, among other techniques. A great deal of knowledge has been obtained about the binding energies and band structures of these states on a variety of surfaces.[1] Recent progress in scanning tunneling microscopy (STM) has revived the interest in some of these states as they were found to form standing waves in the vicinity of defects like adsorbates and step edges.[2–4] The states of interest here are the Shockley-type surface states on the noble metal (111) surfaces. These states are distinguished by their almost perfectly parabolic dispersion relations.

Having observed such standing waves, the next step was to build structures on the surface in order to create boundary conditions. One way of doing this involves the handling of individual atoms by means of an STM tip, first using Xe atoms[5] and later arranging Fe atoms on a Cu(111) surface into circular "quantum corrals"[6] as well as into other shapes. A variety of other atomic species was used as well. Another type of waveguide is provided by step edges. Advances in the techniques of surface preparation, involving epitaxial techniques and thermal treatment, allow one to influence the shapes of islands and terraces.[7] Standing surface waves have been observed in quantum wires formed by narrow terraces on a stepped Au(111) surface, as well as on small islands on Ag(111).[8] These achievements make it possible to view the surface as a two-dimensional nanoscale quantum laboratory in which the surface state is subjected to boundary conditions on a length scale where quantum coherence prevails. In contrast to semiconductor heterostructures, where the transport properties through the device are of primary concern, STM allows the direct observation of the electronic wave functions themselves (or at least, their square moduli). Interesting phenomena can be observed, e.g., for a stadium shape, where quantum chaos is expected.[9]

However, none of the scattering structures mentioned above are ideal reflectors of electrons. Leakage occurs both across the scatterer into the surface state on the other side, and into the bulk of the crystal. This unsatisfactory state of affairs has stimulated experimental as well as theoretical efforts to find better confinement structures, and to understand how they work. The behavior of the quantum corral has been calculated, replacing the ring of adsorbates by a scattering potential of δ function shape.[10] Recently, Crampin[11] has developed a formalism to treat local surface defects in the framework of the layer–Korringa-Kohn-Rostoker (LKKR) method.

In the present work, we want to understand the scattering mechanism of the Cu(111) surface state at a straight row of adsorbates. Numerical results are obtained for a periodic array of rows, using various types of atoms. From the band structure of the periodic array, we draw conclusions about the scattering behavior of one individ-

0163-1829/94/50(24)/18607(14)/$06.00

ual row. The paper is organized as follows. In Sec. II we discuss the problem qualitatively. Section III presents the results of numerical calculations, and in Sec. IV, these results are interpreted in terms of a one-dimensional band structure. The results are drawn together in the concluding Sec. V.

II. QUALITATIVE CONSIDERATIONS: COUNTING STATES

Consider the scattering of a surface state by an object which is of finite size in one direction along the surface (x, say) but which extends to plus-minus infinity in the other direction, y. An example would be a straight row of adatoms, or a step edge. Let us first assume that this scatterer is close packed along the y direction so the unit cell size in y is not increased. This implies that the y component of the Bloch wave vector, k_y, is conserved in the scattering. Therefore, the surface state can only couple with other states which have the same k_y. This situation is visualized in Fig. 1(a). It shows a constant-energy surface, given by the band structure of the bulk of a crystal. A neck in the constant-energy surface causes a projected band gap in which a surface state can exist, indicated by the circle inside the neck in Fig. 1(a). An example would be Cu, choosing the (111) direction as the z axis and ignoring the necks pointing in the directions other than $\pm z$. Since k_y is conserved, the scattering process has to happen within a plane k_y =const cutting through the constant-energy surface, thus generating a constant-energy line. In the presence of a surface, the bulk states at k_z and $-k_z$ combine to form a standing wave, so we need only positive k_z to label our bulk states (complications arising from more than one band are not considered here). The corresponding constant-energy line is shown in Fig. 1(b) for normal incidence, i.e., $k_y = 0$. The k vector of the surface state has a complex z component, so it decays into the bulk.[12] Only Re(k) is shown in Fig. 1(b). In the absence of the adsorbed scatterer, all the states depicted in Fig. 1(b) are orthogonal because they are Bloch states with different k_x. If we now switch on our scatterer, the periodicity along the x direction is broken and all the states in Fig. 1(b) can couple to each other. We denote surface states with positive (negative) k_x as $\psi_s^{\pm}$ and bulk states as $\phi_j^{\pm}$. Both are eigenstates of the Hamiltonian of the crystal in the absence of any adsorbates. The index j is understood to be continuous for a semi-infinite crystal, while it would be discrete for a crystal of finite thickness. A surface state ψ_s^+ coming in from the left and hitting the scatterer gives rise to the following state:

$$\psi = \begin{cases} \psi_s^+ + r\,\psi_s^- + \sum_j c_j^-\,\phi_j^- \;, & x < -x_0 \\ t\,\psi_s^+ + \sum_j c_j^+\,\phi_j^+ \;, & x > x_0. \end{cases} \tag{1}$$

This equation describes the wave function outside of the range of the scattering potential, denoted by $\pm x_0$. The sum over j covers all outgoing bulk states, i.e., all $k_x < 0$ if $x < -x_0$, and all $k_x > 0$ if $x > x_0$. For the purpose of confining an electron by means of added rows, one would like the reflection coefficient r to be as large as possible. The transmission coefficient t causes escape of the electron into a surface state on the other side of the obstacle, while the factors $c_j^{\pm}$ give rise to a loss of electrons into the bulk. The results of Secs. III and IV indicate that in most cases of interest, there is considerable scattering both across the scatterer and into the bulk.

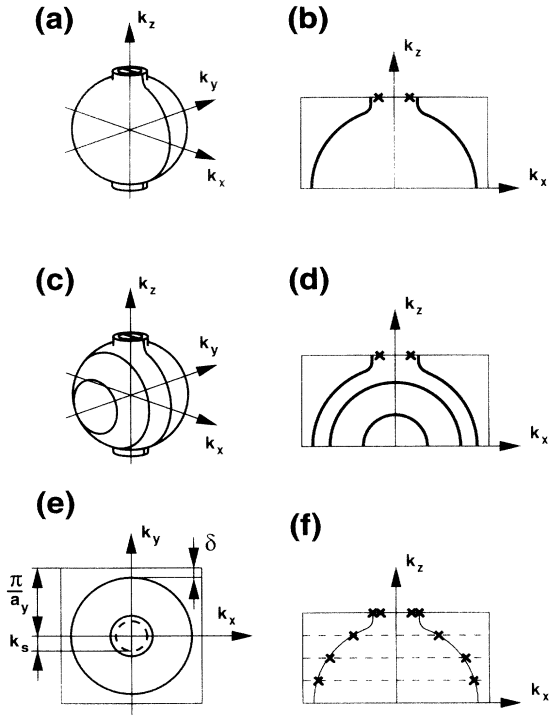

FIG. 1. (a) A constant-energy surface of a metal which supports a surface state. The surface state resides in the surface band gap that exists inside the neck in a vertical projection. It is indicated by a circle within the neck. (b) The constant-energy line generated from (a) by setting k_y =const=0. The crosses indicate the real part of the k vector of the surface state. (c) The constant-energy surface, showing cuts at $k_y = k_{y0} + l\Delta k_y$ =const which arise from the supercell periodicity of the scatterer. (d) The constant-energy lines corresponding to case (c). (e) Top view of the constant-energy surface. The surface state is indicated by the dashed circle. (f) If the crystal is a slab of finite thickness, only discrete values of k_z are allowed, displayed as the horizontal dashed lines. Thus, only a finite number of states are coupled to each other, indicated by the crosses.

Figure 1 and Eq. (1) provide the framework for the following discussion. It will be assumed that all the $c_j^{\pm}$ coefficients scattering into the bulk are of comparable magnitude. The most important influence on the scattering rate is then the number of outgoing states that an incoming state can scatter into.

A. Less than close-packed rows

Suppose that there is an atom adsorbed every M unit cells along the y direction. A supercell of size M causes

the reciprocal lattice to shrink by the same factor, so a state with a certain k_y can now couple to

$$k_{yl} = k_y + l\,\Delta k_y, \tag{2}$$

where

$$\Delta k_y = g_y/M, \tag{3}$$

where g_y is the shortest reciprocal lattice vector of the substrate:

$$g_y = \frac{2\pi}{a_y}. \tag{4}$$

In other words, the incoming surface state is Bragg scattered, so the number of outgoing channels increases. The wave functions and the scattering factors now carry an extra label l from a Bragg reflection by $l\Delta k_y$, so we have surface states $\psi^{\pm}_{s,l}$, bulk states $\phi^{\pm}_{jl}$, and scattering factors r_l, t_l into the surface state and $c^{\pm}_{jl}$ into the bulk.

Let us first consider the limit of large M, i.e., sparse rows. Figures 1(c) and 1(d) show that there are now several cuts through the constant-energy surface separated by Δk_y, which means more states to couple to. However, this does not mean that the scattering rate increases, because by increasing M the scatterer is diluted, reducing its overall effect. The scattering factors go roughly like $1/M$ which can be seen, e.g., from the definition of the T matrix as the matrix element of the scattering potential between the incoming state and the full scattering solution.[13] The volume integral implied in this definition will scale roughly like the number of atomic potentials that we integrate over. For large M, the number of available states goes linear with M. This applies both to bulk states and to surface states (see Appendix A). The wave function for an incoming surface state ψ^{+}_{s0} takes the form

$$\psi = \begin{cases} \psi^{+}_{s,0} + \sum_l r_l\,\psi^{-}_{s,l} + \sum_{jl} c^{-}_{jl}\,\phi^{-}_{jl}\ , & x < -x_0 \\ \sum_l t_l\,\psi^{+}_{s,l} + \sum_{jl} c^{+}_{jl}\,\phi^{+}_{jl}\ , & x > x_0. \end{cases} \tag{5}$$

We now look at $|\psi|^2$. Since this is a rather mixed-up quantity, we will average it over the y coordinate, that is, parallel to the scatterer. All the wave functions $\psi^{\pm}_{s,l}$, $\phi^{\pm}_{lj}$ are Bloch eigenfunctions of the unperturbed surface, so they are orthogonal for different k_y. Therefore, one of the double summations over l disappears. We end up with

$$\begin{aligned} \overline{|\psi|^2} = \overline{|\psi^{+}_{s,0}|^2} &+ \sum_l |r_l|^2\ \overline{|\psi^{-}_{s,l}|^2} + \sum_{jj'l} c^{-*}_{jl}\ c^{-}_{j'l}\ \overline{\phi^{-*}_{jl}\phi^{-}_{j'l}} \\ &+2\,\mathrm{Re}\left[r_0\ \overline{\psi^{+}_{s,0}{}^{*}\psi^{-}_{s,0}} + \sum_j c^{-}_{i0}\ \overline{\psi^{+}_{s,0}{}^{*}\phi^{-}_{j,0}} \right. \\ &\left. + \sum_{jl} r^{*}_{l}\ c^{-}_{jl}\ \overline{\psi^{-}_{s,l}{}^{*}\phi^{-}_{jl}} \right], \quad x < x_0 \end{aligned} \tag{6}$$

and a similar expression for $x > x_0$. The overbars indicate averaging over y.

The number of Bragg reflections (labeled by l) is proportional to the supercell size M. Each term in the sum over l involves two scattering factors which scale as $1/M$ each. Thus, $\overline{|\psi|^2}$ is given by the unperturbed density $\overline{|\psi^{+}_{s,0}|^2}$, plus a scattered density that scales as $1/M$. This $1/M$ behavior holds for both the bulk and surface contributions so the bulk-to-surface ratio is independent of M. As M becomes very large, we reach the limit of a single adsorbed atom with a scattered density around it that does not depend on M anymore. In this limit, the y average of the scattered density scales exactly as $1/M$.

In the opposite limit of small M (dense rows), the ratio of the bulk to the surface contributions is no longer independent of M. An incoming electron can be Bragg scattered by multiples of $2\pi/(Ma_y)$. With the Cu(111) surface in mind, assume a constant-energy surface which does not quite touch the BZ boundary, as in Fig. 1(e). Then an electron in a surface state can be Bragg scattered into the bulk if

$$M > \frac{2k_{\mathrm{BZ}}}{(k_s + k_{\mathrm{BZ}} - \delta)}\ , \tag{7}$$

where δ is the distance from the bulk band to the BZ boundary, k_s is the radius of the surface state band, and $k_{\mathrm{BZ}} = \pi/a_y$. For Cu(111), that may not yet be possible for $M = 2$, depending on the energy, but it definitely starts at $M = 3$. That is not true, however, for Bragg scattering of an incoming surface state into an outgoing surface state. The scattering channels into the surface state at $k_y + l\Delta k_y$ only become available for $M > g_y/(2k_s)$. For the Cu(111) surface, k_s is comparatively small so $M \geq 6$ at the Fermi energy.

The closest distance between adjacent adatoms that has been achieved experimentally by manipulation with a STM is 9.5 Å.[9] With a nearest-neighbor distance of 2.55 Å for Cu, this corresponds to $M = 3.72$, so for our discussion, $M = 4$. In this case, there are already several Bragg channels open into the bulk, but Bragg scattering into the surface state is not yet possible. Thus, the relative importance of bulk scattering over surface scattering is enhanced compared to the dense limit. It is, however, less than in the sparse (single-atomic) limit for a band structure like the one considered here.

It should be stressed that these considerations apply to straight rows only. Other shapes will cause more complicated interference patterns for which the bulk-to-surface ratio of the scattering may reach that of the single adsorbate.

B. Finite thickness of the crystal

It has been proposed[9] that the use of a thin film could reduce the number of bulk states that the surface state can couple to, eventually switching off the scattering into the bulk altogether. We discuss this situation for a close-packed scatterer, thereby avoiding the complications due to Bragg scattering. Thus Eq. (1) applies, where the index j of the bulk states is now genuinely discrete. The bulk states are quantum-well states, their wave vectors

perpendicular to the surface are given by the requirement of constructive interference:

$$2k_z N a_z + \eta_S + \eta_I = j\ 2\pi\ , \tag{8}$$

where N is the thickness of the film in monolayers (ML) and a_z is the lattice constant in the z direction. The phase shifts η_S and η_I arise from the reflections at the surface and at the underlying interface. The discretization of k_z means that there are only isolated points on the constant-energy line that are coupled together, as shown in Fig. 1(f). The minimum thickness is one ML, in which case the separation of two k_z values becomes a maximum:

$$(\Delta k_z)_{\max} = \pi/a_z = k_{\mathrm{BZ}}. \tag{9}$$

Here, k_{BZ} denotes the Brillouin zone boundary in the z direction. Thus, whatever the phase shifts η_S and η_I, there is at least one value of k_z available for the bulk states. This is also clear from the fact that a single monolayer of a metal must have states for its valence electrons, and they will not all be contained in the surface state. Thus, there will be a bulk state around the Fermi energy, no matter how thin the layer.

As to the surface state, it can only exist if there is a band gap, i.e., there must be a "bulk" of sufficient thickness so that the band gap, which is a consequence of the bulk band structure, can form. The surface states of interest here, like those on the noble metal (111) surfaces, have a rather large penetration depth. Calculations show that, e.g., for a thin layer of Ag on Pd(111), a thickness of eight ML is required for the surface state to be fully developed.[14] The same behavior and order of magnitude have been found experimentally on thin films of Ag(111) and Au(111).[15] If the film thickness is less than that, the surface state will feel the presence of the interface. If the film has been grown on an insulating substrate, this interface is repulsive and the surface state is likely to shift up in energy. If the substrate is a metal, then the surface state will turn into a resonance and couple to the bulk even without a scatterer on top.

So there will be bulk states available in all practical situations. However, their number is greatly reduced as compared to the semi-infinite crystal. In order to estimate the effect of this on the reflectivity, we adopt a simplified situation. The metallic layer is modeled as a free-electron quantum well with hard walls. The assumption of a free-electron dispersion relation is not at all bad in the Cu s band which is the band of interest here. Since k_y is conserved, we consider a two-dimensional system with x and z as the horizontal and vertical coordinates. At a given energy E, the eigenstates of this quantum well are given by

$$\phi_j^{\pm}(x,z) = \sqrt{\frac{2}{L}}\ \sin\left(j\frac{\pi}{Na_z}z\right)\ e^{\pm iK_{xj}x}\quad , \tag{10}$$

$$K_{xj} = \sqrt{2E - \left(j\frac{\pi}{Na_z}\right)^2}\quad . \tag{11}$$

These states play the role of the bulk states. A quantum well of this sort does not possess any surface states, but we will include them in the model nevertheless. Thus, we have surface states

$$\psi_s^{\pm}(x,z) = \chi(z)\ e^{ik_x x}\quad . \tag{12}$$

The function $\chi(z)$ is real and drops exponentially into the vacuum region as well as into the bulk. The normalization is chosen to correspond to that of the $\phi_j^{\pm}$:

$$\int_{-\infty}^{\infty} dz\ |\chi(z)|^2 = 1\ . \tag{13}$$

We now consider the currents flowing along the quantum well. The current density of a state ψ is given by $j_x = \mathrm{Im}\,(\psi^*\nabla_x\psi)$ in atomic units ($e = \hbar = m_e = 1$), and the current $I_x = \int j_x dz$. Thus, the surface states $\psi_s^{\pm}$ carry a current of $I_x = \pm k_x$ while the bulk states $\phi_j^{\pm}$ carry a current of $I_x = \pm K_{xj}$. The complete scattering state described in Eq. (1) is a linear combination of these states. It possesses a current which is the sum of the individual currents, plus interference terms between the surface states and the bulk states:

$$I_x = k_x(1-|r|^2)\ -\ \sum_j K_{xj}\ |c_j^-|^2 + \mathrm{Im}\left[\sum_j (\psi_s^+ + r\psi_s^-)^*\ \nabla_x c_j^-\ \phi_j^-\right],\quad x < -x_0. \tag{14}$$

A similar equation holds for $x > x_0$. The cross terms between ψ_s^+ and ψ_s^- vanish, likewise those between ϕ_j^- for different j. For our qualitative discussion, we will also ignore the cross terms between the surface states and the bulk states in Eq. (14). Thus, the inflowing and outflowing currents at the scatterer are

$$I_{\mathrm{in}} = k_x\quad , \tag{15}$$

$$I_{\mathrm{out}} = I_r + I_t + I_{\mathrm{bulk}}\quad , \tag{16}$$

where

$$I_r = I_{\mathrm{in}}|r|^2\quad , \tag{17}$$

$$I_t = I_{\mathrm{in}}|t|^2\quad , \tag{18}$$

$$I_{\mathrm{bulk}} = \sum_j |c_j^-|^2\ K_{xj} + \sum_j |c_j^+|^2\ K_{xj}\quad . \tag{19}$$

Here, I_{bulk} is the current into a bulk of finite thickness. We simplify it by assuming equal coupling strength to each of the bulk modes:

$$\sum_j |c_j^-|^2\ K_{xj}\ \approx\ \sum_j |c_j^+|^2\ K_{xj}\ \approx\ \bar{c}^2\ \sum_j K_{xj}. \tag{20}$$

We now look at a thick layer for which the current scattered into the bulk has saturated to its asymptotic value. For large N, we can replace the sum over j by an integral and evaluate it analytically. The number of running modes, $j_{\max}$, is given by $j_{\max} = \mathrm{Int}(\sqrt{2E}Na_z/\pi)$. The sum over the K_{xj} now becomes

$$\sum_j K_{xj} = \sqrt{2E} \sum_{j=1}^{j_{max}} \sqrt{1 - \left(\frac{j\pi}{\sqrt{2E}Na_z}\right)^2} \rightarrow \frac{ENa_z}{2}, \quad (N \text{ large}). \tag{21}$$

Thus, the current for large N is given by

$$I_{\text{bulk},\infty} = \bar{c}^2 \, ENa_z \, . \tag{22}$$

$I_{\text{bulk},\infty}$ is independent of N so the $\bar{c}^2$ must behave as $1/N$. This behavior is a consequence of the normalization that we have chosen for our bulk wave functions. However, apart from this, we assume that the scattering at the adsorbates does not depend on N, i.e., $\bar{c}^2 = c_0^2/N$, where c_0 =const.

The current into the bulk for a finite N now takes the form

$$I_{\text{bulk}} = I_{\text{bulk},\infty} \frac{1}{NEa_z} \sum_j K_{xj}. \tag{23}$$

The conservation of charge $I_{\text{in}} = I_{\text{out}}$ takes the following form, using the probabilities of reflection $R = |r|^2$, transmission $T = |t|^2$, and absorption (scattering into the bulk) A:

$$R + T = 1 - A, \tag{24}$$

$$A = \frac{c_0^2 E a_z}{k_x} \frac{I_{\text{bulk}}}{I_{\text{bulk},\infty}}. \tag{25}$$

The ratio $I_{\text{bulk}}/I_{\text{bulk},\infty}$ is shown in Fig. 2 for parameters suitable to describe the Cu(111) surface at the Fermi energy E_F. The zero of the energy was taken at the bottom of the s band, so that $E_F = 0.346H$ in this calculation.[20] From the same source, $a_z = 3.9$ a.u. It can be seen from Fig. 2 that the scattering into the bulk is significantly reduced only for very thin layers ($N = 1$ or 2). As outlined above, several monolayers are required to allow the surface state to form. For $N \geq 5$, the scattering into the bulk is only reduced by 11% or less, compared to the semi-infinite limit. This result indicates that using a thin film instead of a semi-infinite crystal is unlikely to reduce the scattering rate into the bulk by a great amount. The absolute rate of scattering into the bulk is controlled by the constant c_0 which is determined by the scattering behavior of the actual scatterer.

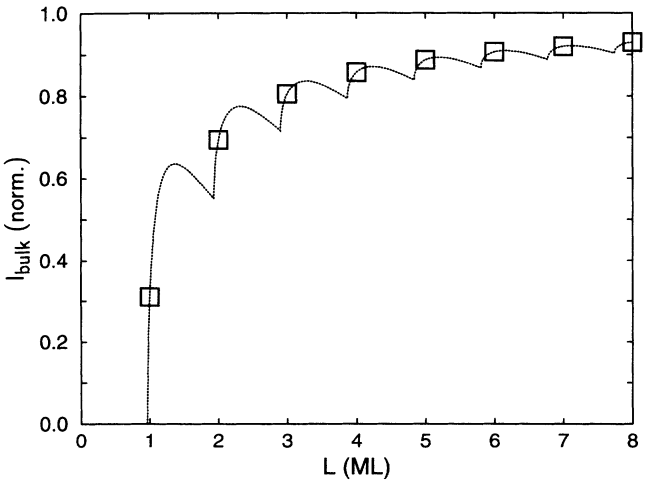

FIG. 2. This graph shows $I_{\text{bulk}}/I_{\text{bulk},\infty}$, i.e., the current of electrons scattered from a surface state into a layer of finite thickness, normalized to the limit of a thick layer. Parameters pertaining to the Cu(111) surface have been used (see text). L is the thickness of the layer. The squares indicate multiples of one monolayer.

III. NUMERICAL CALCULATIONS

The previous section allowed some qualitative insight concerning the scattering of a surface state by a row of adatoms, but it contained scattering parameters about which very little could be said. In particular, there was no information about the absolute magnitude of the surface-to-bulk scattering $c_j^{\pm}$ and the the surface-to-surface scattering r, t. In this section, we will try to calculate quantitatively the strength of this scattering. However, the problem of a single added row or step edge is a formidable one so instead we look at a supercell geometry, that is, a regular array of added rows. Thus, we have changed the nature of the problem and we can no longer think in terms of ingoing and outgoing waves because there is no "outside," i.e., no region on the surface without any adsorbates. Instead, we want to draw conclusions in an indirect way from the band structure of this periodic system. The idea is that a surface state in the presence of an array of added rows will be coupled to the bulk. Therefore, strictly speaking, it is not a surface state any longer, but a surface resonance with a finite lifetime at the surface. In the surface band structure, it will no longer show up as a δ function in the energy, as with a genuine surface state, but it will be broadened to a certain extent. From this, we can get information about the strength of the scattering into the bulk. By performing band structure calculations for a variety of added atoms, we hope to identify the best candidates for surface state engineering, that is, those with maximum reflectivity and minimum transparency.

A. Numerical method

The electronic structures were calculated using the layer–Korringa-Kohn-Rostoker (LKKR) method.[16] In this approach, layers of atoms are represented by layers of spherically symmetric muffin-tin potentials. Each layer is characterized by its transmission and reflection coefficients. Two layers can be coupled to obtain the scattering coefficients of a double layer. These in turn are coupled in succession to get four, eight,. . . ,2^n layers, a technique called layer doubling. In this way, the reflection coefficient of a semi-infinite crystal can be obtained. A small imaginary part has to be added to the energy in order to ensure convergence.[16]

In order to describe the surface band structure, we make use of the local density of states (LDOS) in the

vacuum close to the surface. The LDOS, $n(\mathbf{r},E)$ is given by

$$n(\mathbf{r},E) = -\frac{2}{\pi}\,\mathrm{Im}G(\mathbf{r},\mathbf{r},E), \tag{26}$$

where the factor of 2 counts spin. The Green's function $G(\mathbf{r},\mathbf{r},E)$ in front of the surface can be written in terms of the vacuum Green's function G_0, plus a part G_s that involves scattering by the surface:

$$G(\mathbf{r},\mathbf{r}',E) = G_0(\mathbf{r},\mathbf{r}',E) + G_s(\mathbf{r},\mathbf{r}',E). \tag{27}$$

Below the zero of energy in the vacuum, only the scattered part G_s will contribute to the local density of states. It is related to the reflection coefficient of the surface, $R_{gg'}(\mathbf{k}_{||},E)$, in the following way:

$$G_s(\mathbf{r},\mathbf{r}',E) = \frac{1}{(2\pi)^2}\int_{\mathrm{BZ}} d^2k_{||} \sum_{g,g'} e^{i(\mathbf{k}_{||}+\mathbf{g})\cdot\mathbf{r}_{||}} \times G_s(\mathbf{k}_{||},\mathbf{g},\mathbf{g}',z,z';E)\; e^{-i(\mathbf{k}_{||}+\mathbf{g}')\cdot\mathbf{r}'_{||}}\,, \tag{28}$$

$$G_s(\mathbf{k}_{||},\mathbf{g},\mathbf{g}',z,z';E) = -\,e^{\kappa^+_g z}\,R_{gg'}(\mathbf{k}_{||},E)\,\frac{1}{\kappa^+_{g'}}\,e^{\kappa^+_{g'}z'}\,. \tag{29}$$

Here, the z coordinate points into the sample, $\mathbf{g},\mathbf{g}'$ are two-dimensional reciprocal lattice vectors, and the decay into the vacuum is given by[17]

$$\kappa^+_g = \sqrt{(\mathbf{k}_{||}+\mathbf{g})^2 - 2E}. \tag{30}$$

The reflection coefficient is one of the central quantities in the layer-KKR method.[16] The Fourier transform of the imaginary part of G_s will be called Γ_s; it is given by

$$\mathrm{Im}G(\mathbf{r},\mathbf{r}',E) = \frac{1}{(2\pi)^2}\int_{\mathrm{BZ}} d^2k_{||} \sum_{g,g'} e^{i(\mathbf{k}_{||}+\mathbf{g})\cdot\mathbf{r}_{||}} \times \Gamma_s(\mathbf{k}_{||},\mathbf{g},\mathbf{g}',z,z';E)\; e^{-i(\mathbf{k}_{||}+\mathbf{g}')\cdot\mathbf{r}'_{||}}\,, \tag{31}$$

$$\Gamma_s(\mathbf{k}_{||},\mathbf{g},\mathbf{g}',z,z';E) = \frac{1}{2i}\Big[G_s(\mathbf{k}_{||},\mathbf{g},\mathbf{g}',z,z';E) - G^*_s(-\mathbf{k}_{||},-\mathbf{g},-\mathbf{g}',z,z';E)\Big]\,. \tag{32}$$

Armed with these quantities, we define $\overline{n}(\mathbf{k}_{||},z,E)$, the local density of states at the distance z from the surface, averaged over the parallel unit cell Ω and separated into contributions from different $\mathbf{k}_{||}$ vectors,

$$\overline{n}(z,E) = \frac{1}{\Omega}\int_{\Omega} d^2r_{||}\; n(\mathbf{r},E) = \int_{\mathrm{BZ}} d^2k_{||}\;\overline{n}(\mathbf{k}_{||},z,E), \tag{33}$$

$$\overline{n}(\mathbf{k}_{||},z,E) = -\frac{1}{2\pi^3}\sum_{g}\Gamma(\mathbf{k}_{||},\mathbf{g},\mathbf{g},z,z;E)\,. \tag{34}$$

Viewed as a function of $\mathbf{k}_{||}$ and E for constant z, $\overline{n}(\mathbf{k}_{||},z,E)$ represents the surface band structure. In the literature on the electronic structure of surfaces, the band structure is usually displayed as a gray-shaded area wherever there is a continuum of bulk states, while surface states are indicated by discrete lines. In our representation, $\overline{n}(\mathbf{k}_{||},z,E)$ is a smooth continuous function within the bulk continuum, it is zero in a surface band gap, and a surface state causes a δ function peak as a function of E. From the value of $\overline{n}(\mathbf{k}_{||},z,E)$, we can tell not only whether a particular point in the $(\mathbf{k}_{||},E)$ plane contributes to the LDOS, but also how much.

As mentioned before, we have to add a small imaginary part to the energy in order to ensure convergence of the layer-doubling procedure in the LKKR formalism. This leads to a broadening of the δ function into a Lorentzian shape with a full width at half maximum of $2\,\mathrm{Im}E$, while the tail of the Lorentzian causes $\overline{n}(\mathbf{k}_{||},z,E)$ to be small but nonzero inside the band gap. The surface state shows up as a sharp ridge in a contour plot in the $(\mathbf{k}_{||},E)$ plane.

B. Calculations and results

Previous experience in our group suggested that p elements like sulfur and carbon, which are generally considered as dirt in surface science experiments, are strongly repulsive scatterers of electrons so they should be interesting candidates for the task at hand. The element actually used in Refs. 6, 9 was Fe. We, therefore, performed calculations for rows of adsorbed Cu, Fe, C, and S in a 6×2 supercell geometry, with the added rows in the $(\bar{1}01)$ direction [Fig. 3(a)]. In addition to that, the presence of step edges was simulated by looking at a missing-row geometry in a 6×1 unit cell, with the missing row(s) again in the $(\bar{1}01)$ direction [Fig. 3(b)].

The S and C potentials were reused from earlier investigations of the adsorption of these atoms on the Ni(100) surface.[18,19] In these papers, the potentials were generated by overlapping atomic charge densities, adding an exchange-correlation energy using the Hartree-Fock-Slater X_α scheme and tuning the exchange parameter to match the nickel d-phase shift to that of the Ni bulk. For the adsorbed Fe and Cu atoms, as well as for the bulk, we used self-consistent bulk KKR potentials.[20] For Fe, the non-spin-polarized case in Ref. 20 was used. The space between the adsorbates was filled with spheres of constant potential, with a muffin-tin radius equal to that of the bulk Cu. The constant potential inside the spheres was adjusted so that the surface state on the clean Cu(111) surface, covered with one layer of empty spheres, occured at the correct binding energy.[21] This required a value of +0.527 Hartree ($1H$=27.2 eV). On top of the layer of empty spheres, a step potential was used to describe the vacuum potential, with a work function of 5 eV. Together with the Fermi energy of the bulk Cu which is $0.314H$ relative to the constant interstitial potential,[20] this gives a step height of $0.498H$. Since our potentials are not determined self-consistently in the framework of density functional theory, we cannot be absolutely sure that what we call, e.g., Fe will really behave

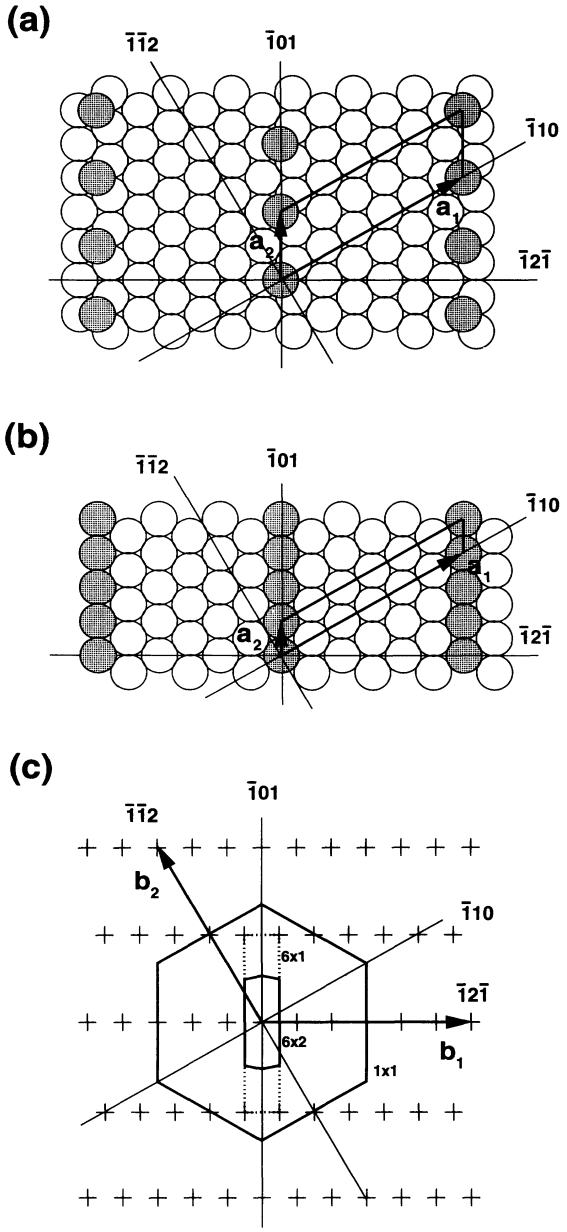

FIG. 3. (a) The geometry of the added rows used in the calculations. The unit cell is 6×2, and the unoccupied adsorption sites are filled with empty spheres (not shown). Adsorbates are indicated by shaded circles. (b) The missing-row geometry with a 6×1 unit cell. The missing atoms are replaced by empty spheres (indicated by shaded circles). (c) The Brillouin zones corresponding to (a) and (b). The large hexagon corresponds to the clean fcc (111) surface.

like adsorbed Fe. Thus, if the results were strongly dependent on the assumed input potential, they would not mean very much. In practice, it turns out that the results that we are most interested in, namely, the broadening and the dispersion of the surface state, are quite robust. They seem to be rather unaffected by the detailed features of the adsorbed potential.

The results of the band structure calculations are summarized in Fig. 4. The bands are shown in a direction in $\mathbf{k}_{||}$ space perpendicular to the added rows [see Fig. 3(c)]. There are two types of behavior. First, added rows of Cu and Fe act as attractive scatterers. The surface state is pulled down in energy and splits up at the Brillouin zone (BZ) boundary. It survives as a sharp resonance near the bottom of the first backfolded band, but everywhere else it is strongly coupled to the bulk, in particular, in the lowest band. In the case of Cu, the lowest band has dropped below −1 eV which is the lower boundary of the figure. The case of C and S is quite different. Now the lowest band is pushed up in energy, indicating that these atoms are effectively repulsive, as we expected them to be. The broadening of the surface resonance is substantial throughout most of the BZ except close to the boundary. The next higher band has been pushed up and broadened beyond recognition.

In addition to these cases, calculations were done for the missing-row 6×1 supercell geometry shown in Fig. 3(b). For the surface state in the strip between two missing rows, the boundary condition looks much like a step edge as seen from the higher terrace. The resulting band structure (not shown) corresponds to a repulsive scatterer and resembles the right two panels in Fig. 4, except that the broadening of the band is smaller.

Figure 5 shows the spectral form of the lowest band at the $\bar{\Gamma}$ point for all cases calculated. It appears that Fe and step edges produce the least broadening, and that S and C are worst. Cu is in between and has a somewhat irregular spectral shape. The energies and the broadening of the bands in Fig. 4 cannot all be obtained by fitting Lorentzians because of the asymmetric line shapes. We have to take care of the influence of the bulk band structure by allowing for a background phase shift δ_0, thus generating a Fano line shape:[22]

$$n(E) = c_0 + c_1 \sin^2(\delta_0 + \delta_r), \tag{35}$$

$$\delta_r = -\arctan \frac{\frac{1}{2}\Gamma}{E - E_r}. \tag{36}$$

Fitting this curve to the spectral shapes depicted in Fig. 5, we can extract the complex energy of the pole, $E_r - i\Gamma/2$. The results of this fit are listed in columns 2 and 3 of Table I.

IV. ONE-DIMENSIONAL COMPLEX BAND STRUCTURES

Complicated as the band structures in the last section may be, the behavior of the surface state can be understood in rather simple terms using a one-dimensional model. In Appendix B, a method is discussed to calculate the band structure of a one-dimensional array of scatterers. The scatterers are assumed to be potential wells or barriers with a constant complex potential, separated by zero-potential regions. An effective mass $m^* \neq 1$ is used in the model. Because of the complex potential, the scatterers are "leaky" which simulates the coupling to an extended system like the bulk of a crystal.

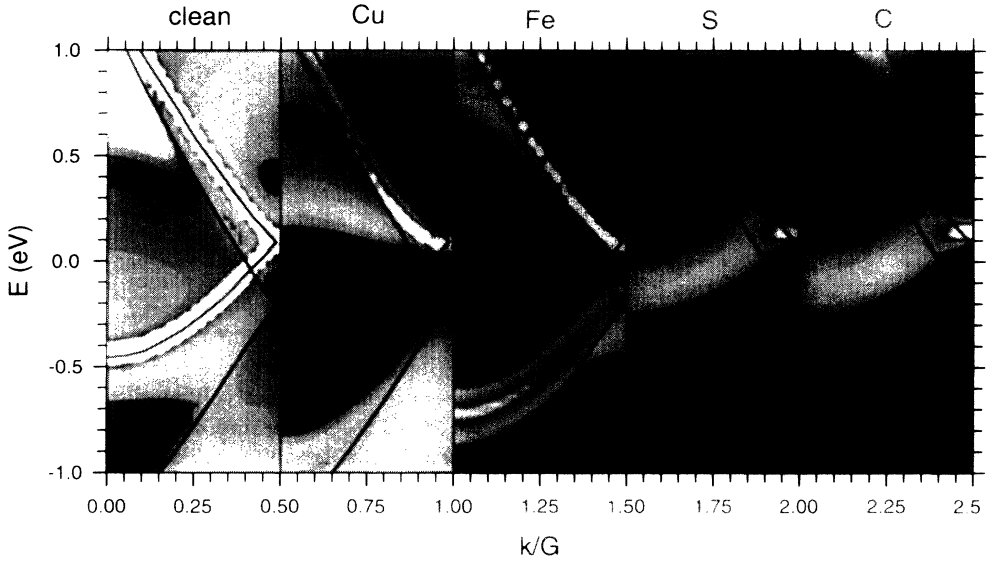

FIG. 4. The surface band structures of the Cu(111) surface with added rows along $\bar{1}01$ in a 6×2 geometry. The direction in k space is $\bar{1}2\bar{1}$ perpendicular to the rows. Contour plots of $\overline{n}(\mathbf{k}_{||}, z = 0, E)$ are shown (see text). Within each panel, $\overline{n}(\mathbf{k}_{||}, z, E)$ has been rescaled. The far left panel shows the clean Cu(111) surface, with the surface state folded back due to the sixfold supercell. In all panels, the positions of the "clean" surface state and of the bulk band edge are indicated as bold black lines. The lumpy appearance of the surface state is due to the finite grid used in the calculation. S and C show an irregularity at $\mathbf{k}_{||}/G \approx 0.4$ and $E \approx 0.6$ eV, which is due to convergence problems in the calculation of the KKR structure constants.

A. Typical cases

We discuss two cases, an attractive potential and a repulsive one. The geometry is chosen as $a = 13$ Å and $b = 2.5$ Å which comes close to the added rows in Sec. III. The scattering potentials are $W = \pm 2$ eV, $\mathrm{Im}V = -1$ eV,

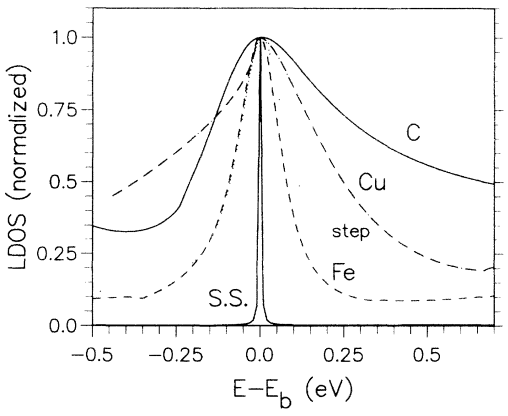

FIG. 5. The peak in the lowest band at the $\bar{\Gamma}$ point. The quantity $\overline{n}(\mathbf{k}_{||} = 0, z = 0, E)$ is shown as a function of E relative to the bottom of the band, E_b. All peaks have been rescaled to the same height, but their width in energy has not been changed. The curve labeled "step" refers to a 6×1 unit cell in which two adjacent atoms are missing in the top layer, i.e., a double missing-row geometry. The case of S (not shown) is nearly identical to C. The surface state of the clean surface is labeled SS. Its linewidth is twice the imaginary part of the energy in the layer-KKR calculation, which was 0.0027 eV.

and the effective mass corresponds to that of the Cu(111) surface state,[21] $m^* = 0.46$.

In the case of an attractive potential, all the bands are pulled down as shown in Fig. 6(a). The lowest band has a very large $\mathrm{Im}E$, indicating that its lifetime is very short. In comparison, the higher bands are doing better, at least near their low energy edges. The high energy sides of the bands again suffer rapid decay. A look at the wave functions explains this behavior [Fig. 7(a)]. The lowest band comprises essentially bound states inside the attractive scatterer, i.e., core states. A particle in such a state spends most of its time in the absorbing region, thus the high damping rate. As we cross the band gap into

TABLE I. The parameters of the scattering potential necessary to reproduce the lowest eigenvalue at the $\bar{\Gamma}$ point of the LKKR band structures (see text). Columns 2 and 3 show the eigenvalue E to be fitted ($E_0 = -0.44$ eV is the energy of the surface state with no adsorbates), columns 4 and 5 show the real and imaginary parts of the scattering potential. The unit cell size is 13.2 Å and the scatterers are 2.2 Å in width. All energies are measured in eV.

Adsorbate	$\mathrm{Re}(E) - E_0$	$\mathrm{Im}(E)$	$\mathrm{Re}(V)$	$\mathrm{Im}(V)$
Cu	-0.59	-0.22	-2.3	-0.59
Fe	-0.28	-0.077	-1.29	-0.28
S	0.21	-0.20	0.93	-1.95
C	0.23	-0.19	1.12	-2.04
M1[a]	0.17	-0.09	1.17	-0.93
M2[b]	0.22	-0.09	1.75	-1.1

[a]One missing row.
[b]A double missing row.

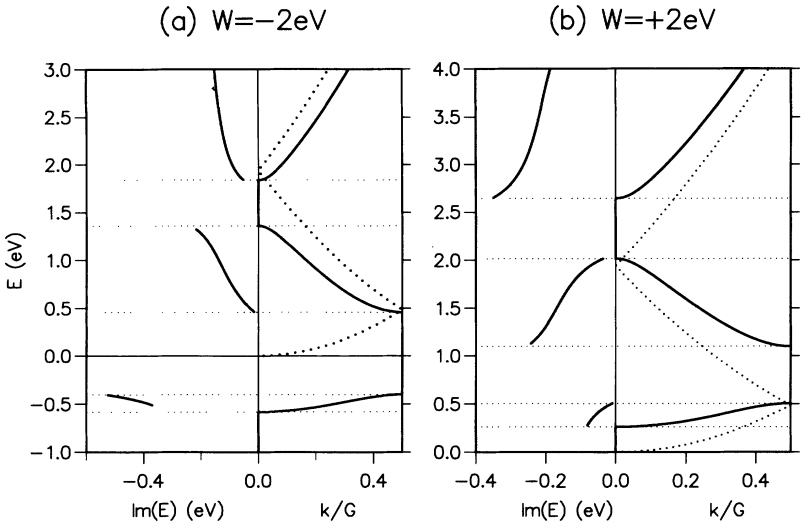

FIG. 6. One-dimensional band structures of a regular array of absorbing scatterers. The right panels show the energy bands. The heavy dotted line indicates the free particle dispersion relation. The left panels show ImE, which is a measure of the lifetime broadening of the bands. (a) Attractive scatterers, $W = -2$ eV. (b) Repulsive scatterers, $W = +2$ eV. In both cases, Im$V = -1$ eV. Note that the energy axis in (b) is shifted relative to (a).

the first band, the character of the wave function changes from bonding into antibonding [panel 3 in Fig. 7(a)]. This wave function hardly enters the absorbing region at all so its damping is also very small. As we move up along the second band, some weight returns to the absorbing region so the damping increases.

The repulsive potential shows the opposite behavior. All the bands are pushed up, the lowest band is not very strongly damped, and the states generally have a longer lifetime near the top of a band [Fig. 6(b)]. The wave functions show why: The lowest band now forms a standing wave between the repulsive scatterers, thus avoiding the absorbing region. The bonding-antibonding character here refers to the area between the scatterers. Thus at the bottom of the second band, which is antibonding, the wave function is pushed into the absorbing region, increasing its damping.

B. Comparison with surface band structures

The generic behavior of the bands in Fig. 6 is already reminiscent of the LKKR band structures in Fig. 4. To see how far these similarities go, the parameters of the one-dimensional model (the real and imaginary potentials within the scatterers) were adjusted such that the resulting lowest eigenvalue at $\overline{\Gamma}$ coincided in position and lifetime broadening with the one from the LKKR calculation. The lattice constant was taken as $a = 13.2$ Å and the width of the scatterer as $b = a/6$. The required parameters are listed in Table I.

The main result is that the transition and noble metal adsorbates act as attractive scatterers, and that the p elements are repulsive. Single and double missing rows are also repulsive scatterers. The attractive scatterers have a less absorbing behavior than the repulsive ones. Part

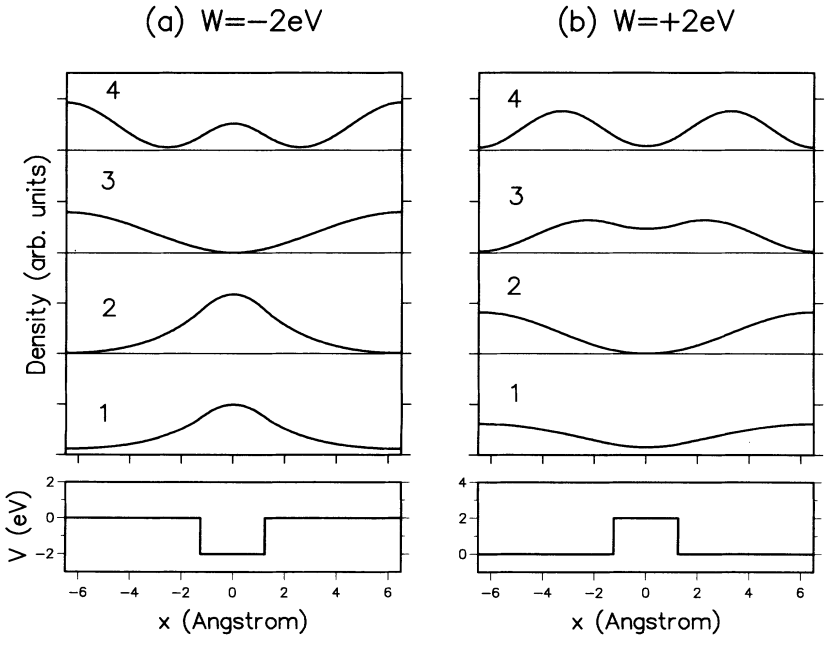

FIG. 7. The square moduli of the Bloch wave functions of a one-dimensional band structure, shown in one unit cell with the scatterer at the center. The real part of the potential is shown in the lower panels. The numbers indicate certain positions in the band structure. 1—bottom of the lowest band, 2—top of the lowest band, 3—bottom of the second band, 4—top of the second band. (a) Attractive scatterers, $W = -2$ eV. (b) Repulsive scatterers, $W = +2$ eV. In both cases, Im$V = -1$ eV.

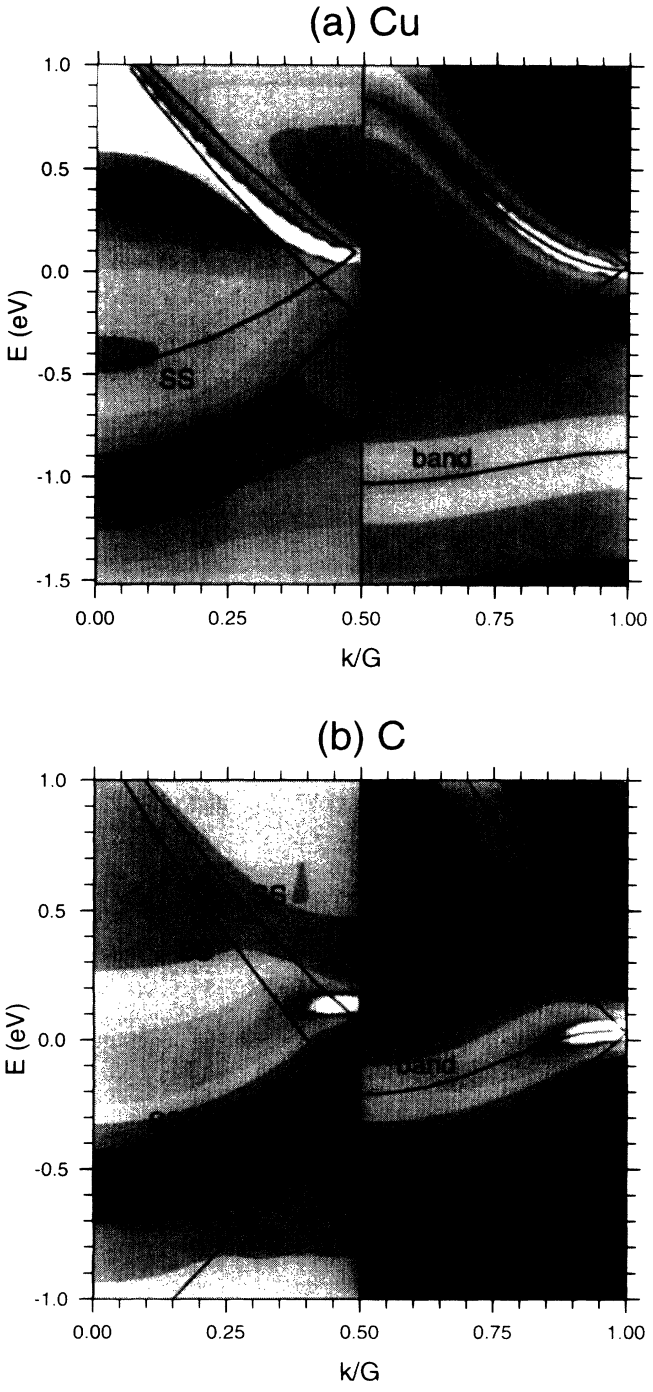

FIG. 8. The surface band structure of the Cu(111) surface with $(\bar{1}01)$ rows of adsorbates in a 6×2 geometry. The bands are shown along $\bar{1}2\bar{1}$ which is perpendicular to the rows. Contour plots of $\overline{n}(\mathbf{k}_{||}, z, E)$ are shown (see text). Left panels: the LKKR results. SS indicates the undisturbed surface state, and BB the bulk band edge. Right panels: the results of a one-dimensional model (see text). "free" indicates the free-electron band, "band" the real part of the energy eigenvalues. The contours have been generated by broadening the bands with a Lorentzian according to their imaginary parts. (a) Adsorbed Cu, (b) adsorbed C. Note that the dark structure at −1.05 eV in the Cu LKKR band structure is a maximum.

of the explanation for this may be found in the argumentation of Sec. II A leading to Eq. (7). The radius of the surface state band, k_s, grows with increasing energy, while the separation δ between the bulk band and the BZ boundary shrinks. Thus, there are more outgoing states available at higher energies. Repulsive scatterers push the bands up to higher energies, where the inequality (7) is true for the case $M = 2$ that we consider here, so there is Bragg scattering into additonal bulk states. This applies for the 6×2 rows of adsorbed S and C, but not for the 6×1 missing-row geometries which are close packed (M=1). Consequently, ImV in the missing-row cases is only about half that of S or C. The attractive scatterers Cu and Fe, on the other hand, pull the bands down into a region where the first Bragg channel for $M = 2$ is closed.

Figure 8 shows two typical examples, Cu and C. Obviously the effect of the added rows on the surface state can be modeled quite well. Fitting the scatterers to reproduce one eigenvalue at one k point, we can reproduce the behavior over the whole range of energies and k vectors considered. Naturally, the bulk bands are absent in the one-dimensional model, but the shifts and the broadening of the surface state are fully captured.

C. A single adsorbed row

The success of explaining the surface band structure in terms of a simple model scatterer is not only nice in its own right, it also allows us to extend our discussion from the periodic array of adsorbed rows to the much more interesting case of a single adsorbed row. The properties of the one-dimensional model scatterer are taken as representative for the more complicated real situation. From the reflection and transmission coefficients r and t (see Appendix B), we can get the *probabilities* of reflection $R = |r|^2$, transmission $T = |t|^2$, and absorption, i.e., scattering into the bulk, $A = 1 - R - T$. The results are shown in Fig. 9 for adsorbates, and in Fig. 10 for missing rows. Clearly, none of these scatterers is a particularly strong reflector of electrons. At the Fermi energy, R is around 30%, except for Cu and a double missing row where it reaches 40% (see Table II). Concerning the loss mechanism, the adsorbates form two distinct groups [Fig. 9(b) and 9(c)]. The transition metals allow the surface state to sneak through and continue on the other side (horizontal loss) but they do not couple strongly to the bulk. Conversely, the p elements are effective barriers horizontally but they send the incoming particle down into the bulk (vertical loss). The missing rows are in between, with the vertical loss being somewhat larger than the horizontal one, especially for the double missing row [Fig. 10(b) and 10(c)].

Experimentally, the scattering rate of adsorbed Fe was estimated to be R=0.25, T=0.25, and A=0.5 (Ref. 9) by fitting a single-phase shift model to the standing waves observed in STM. In our calculation, the values are R=0.24, T=0.5, and A=0.25 (Table II). There is an important difference between the experiment, where the density of the atomic rows corresponded to $M \approx 4$, and our own supercell size of $M = 2$. With our current

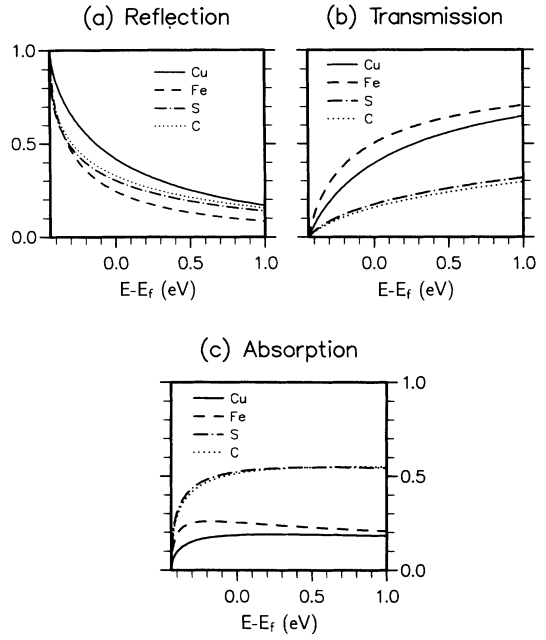

FIG. 9. The probabilities of an electron in a surface state being (a) reflected, (b) transmitted, or (c) scattered into the bulk (absorbed) by a row of adatoms on the Cu(111) surface.

computing setup, the numerical effort for $M = 4$ is prohibitive. From the discussion in Sec. II A, it appears that our calculation has less scattering channels open into the bulk than the experiment, hence the smaller rate of absorption.

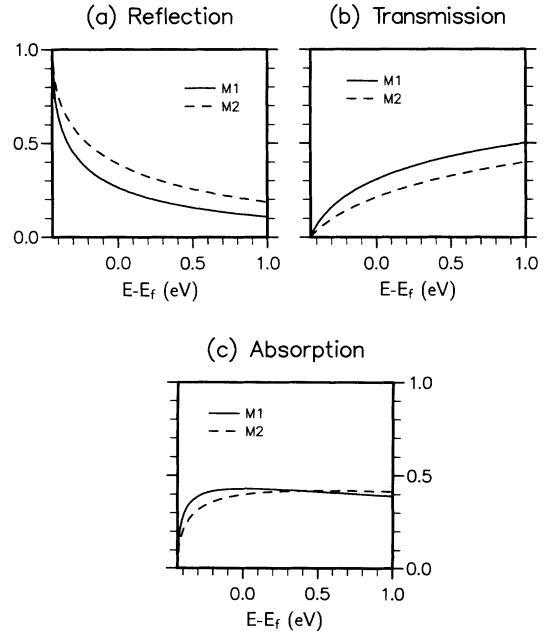

FIG. 10. The probabilities of an electron in a surface state being (a) reflected, (b) transmitted, or (c) scattered into the bulk by missing rows on the Cu(111) surface. M1—a single missing row, M2—a double missing row.

TABLE II. The probabilities of reflection, transmission, and absorption (scattering into the bulk) at the Fermi energy. They were calculated from one-dimensional scatterers which were adjusted to reproduce the LKKR band structure of the surface state (see text).

Adsorbate	Reflection	Transmission	Absorption
Cu	0.42	0.39	0.19
Fe	0.24	0.50	0.25
S	0.30	0.17	0.52
C	0.33	0.16	0.52
M1[a]	0.26	0.31	0.43
M2[b]	0.39	0.21	0.40

[a]One missing row.
[b]A double missing row.

It is clear that these results can only be considered as semiquantitative. The electronic potential of an adsorbate is certainly not equal to that of the same atom in the bulk, nor can an adsorbate be expected to behave in exactly the same way on different surfaces. However, we have looked at a selection of rather different atoms so the variation of the results gives us an indication of the possible error span. The main result is that whatever the adsorbate, the reflectivity will, in general, stay below 50%. Two possible sources of error must be addressed here. The first concerns the vertical position of the adsorbed C, which was assumed on an extended lattice site of the Cu substrate. Carbon is a small atom and it is likely to sit closer to the surface than that. On the Ni(100) surface, the influence of the vertical position of the C on the electronic structure is pronounced. Thus, the LKKR calculation was repeated for a number of vertical displacements of the C from the Cu lattice position, namely, by -0.4 Å, -0.2 Å, $+0.2$ Å, and $+0.4$ Å. Relaxing the C towards the surface is seen to decrease the reflectivity even further (Fig. 11), while it enhances the transmittivity and leaves the absorption into the bulk nearly unchanged. The second problem may arise from the non-spin-polarized treatment of the Fe. Recent work on the scattering properties of this adsorbate indicate that spin polarization is an important factor.[11]

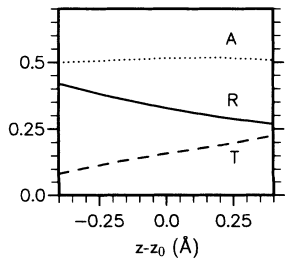

FIG. 11. The effect of altering the vertical position of adsorbed carbon. Positive $z - z_0$ is closer to the surface. R, T, and A are the probabilities of reflection, transmission, and absorption into the bulk, all taken at the Fermi energy.

V. CONCLUSIONS

In this paper, we have investigated the scattering of the surface state on the Cu(111) surface by straight rows of adsorbed atoms, as well as step edges. A layer–Korringa-Kohn-Rostoker (LKKR) formalism was used to obtain the band structures of the surfaces in question. A periodic structure of added rows or missing rows (the latter to simulate step edges) was assumed. Calculations were done for 6×2 superstructures of adsorbed Cu, Fe, S, and C, as well as for 6×1 structures of one and two missing rows. From the band structure of this periodic system of scatterers, the properties of one single scatterer were obtained by fitting a one-dimensional model. This model involves scatterers of quantum-well shape. It allows a remarkably good description of the behavior of the surface state in the presence of the added rows, including the lifetime broadening caused by the coupling to the bulk.

The quality of the band structure calculations suffers from the fact that they were not done self-consistently in the framework of density functional theory. Instead, self-consistent bulk potentials were used for all layers including the topmost one, and the potentials of some adsorbates were constructed by using the $X\alpha$ method. Thus, our results are not fully quantitative. However, we have used a considerable variety of adsorbates so the trends that were identified in the results should be reliable.

The main conclusion from the calculations is bad news for surface state engineering. None of the scatterers investigated shows a reflectivity of more than ca. 40% at the Fermi energy. The scatterers with d character (Cu and Fe) tend to leak mainly horizontally (into the surface state on the other side of the scatterer) while those with p character show predominantly vertical loss (into the substrate). Single and double missing rows are in between.

By counting the states that an electron in a surface state can be scattered into, we obtain some qualitative insight into the problem. For a band structure similar to that of Cu(111), an added row which is less than close packed gives rise to a relative enhancement of scattering into the bulk compared to that into the surface state. The total scattering rate decreases because of the dilution of the scatterer. A supercell of size M switches on additional (Bragg) channels into the bulk for $M \geq 2$ or 3, while Bragg scattering into the surface state becomes available only for $M \geq 6$. The most densely packed rows of adsorbates that have been made in practice so far ($M \approx 4$) are thus in a region of relatively enhanced bulk scattering, and therefore, loss. Step edges, on the other hand, are close packed and do not lead to Bragg scattering, which may be an advantage.

The effect of replacing the semi-infinite substrate by a thin film is considered in a simplified quantum-well model. It is argued that a big reduction of the scattering rate into the bulk is unlikely.

All this suggests that the total confinement of a surface state in a closed structure may not be feasible. However, the results of this paper as well as other theoretical and experimental findings,[9–11] show that the interaction of the surface state with most adsorbates is substantial. Further exploration of these systems both in theory and experiment is highly desirable.

ACKNOWLEDGMENTS

This work was supported by the United Kingdom Science and Engineering Research Council (SERC). G. H. would like to thank Etienne Hofstadter for helpful discussions.

APPENDIX A: NUMBER OF AVAILABLE STATES

In this appendix, we estimate the number of states that a surface state can be scattered into by a row of adsorbed atoms. The adsorbed row can be less than close packed, with one adsorbed atom every M bulk unit cells. We count only states with the same sign of the wave vector k_x, because $k_x > 0$ and $k_x < 0$ are counted separately in the discussion following Eq. (5). Only positive k_z are considered [see Figs. 1(b), 1(d)].

For the bulk states, a spherical constant-energy surface is assumed with radius k. The number of states that an incoming state at k_y can Bragg scatter into is given by cuts through the surface at $k_{yl} = k_{y0} + l\Delta k_y$, where $\Delta k_y = g_y/M$. We set $k_{y0} = 0$. Then each cut gives a circle (or rather, a quarter circle, see above) with the radius

$$k_l = \sqrt{k^2 - \left(\frac{l}{M}\, g_y\right)^2} \,. \tag{A1}$$

The maximum index of the cuts is given by $\pm l_{\max}$:

$$l_{\max} = \mathrm{Int}\left(\frac{Mk}{g_y}\right) \,. \tag{A2}$$

Assuming a constant linear density of states ρ_1 along the constant-energy surface, we get the number of bulk states,

$$N_b = \frac{\pi}{2} k \rho_1 \sum_{-l_{\max}}^{l_{\max}} \sqrt{1 - \left(\frac{l\, g_y}{M\, k}\right)^2} \,. \tag{A3}$$

In the limit of large M, we can convert this into an integral, with the result

$$N_b = \frac{M \rho_1 k^2 \pi^2}{4 g_y} \,. \tag{A4}$$

Thus the number of available bulk states is proportional to the supercell size M, and also to the area of the constant-energy surface.

The number of surface states N_s is given by the number of intersections through the constant-energy line of the surface state in the (k_x, k_y) plane [see Fig. 1(e)]. Assuming a circular shape with a radius k_s, and taking only half of the circle ($k_x < 0$ or $k_x > 0$), we get

$$N_s = \mathrm{Int}\left(\frac{2Mk_s}{g_y}\right) . \tag{A5}$$

This number is again proportional to M.

APPENDIX B: CALCULATING ONE-DIMENSIONAL BAND STRUCTURES

We follow the approach by Ashcroft and Mermin.[23] Consider a one-dimensional periodic array of scattering objects each of which is characterized by its reflection and transmission coefficients, r and t. The scatterers do not overlap, so each scattering potential is confined to a region not larger than the length of the unit cell, a. Atomic Hartree units $e = \hbar = m_e = 1$ are used but the mass of the particle may be an effective mass $m^* \neq 1$. We assume inversion symmetry. For a single scatterer at the origin, we can define two scattering solutions ψ_l and ψ_r which have outgoing boundary conditions at $x \to \infty$ and at $-\infty$, respectively,

$$\psi_l(x) = \begin{cases} e^{iKx} + r\, e^{-iKx}, & x \le -a/2 \\ t\, e^{iKx}, & x \ge a/2 , \end{cases} \tag{B1}$$

$$\psi_r(x) = \begin{cases} t\, e^{-iKx}, & x \le -a/2 \\ e^{-iKx} + r\, e^{iKx}, & x \ge a/2, \end{cases} \tag{B2}$$

$$K = \sqrt{2m^*E}. \tag{B3}$$

The uppercase K denotes the free-electron wave number and must not be confused with the lowercase k which is the Bloch wave vector. The latter is determined by the Bloch condition of the periodic array, Eqs. (B5) and (B6),

$$\psi(x) = A\,\psi_l(x) + B\,\psi_r(x) , \tag{B4}$$

$$\psi(a/2) = e^{ika}\,\psi(-a/2) , \tag{B5}$$

$$\psi'(a/2) = e^{ika}\,\psi'(-a/2) . \tag{B6}$$

From these equations, one can extract the Bloch wave vector k,

$$\cos(ka) = \frac{1}{2t}\left[(t^2 - r^2)\, e^{iKa} + e^{-iKa}\right], \tag{B7}$$

as well as the relative weights of the states $\psi_l(x)$ and $\psi_r(x)$ in the Bloch function,

$$B = -\frac{1}{r}\left(t - e^{i(k-K)a}\right) A . \tag{B8}$$

To be more specific, the scatterers are assumed to be rectangular potential wells or barriers of width $b < a$:

$$V(x) = \begin{cases} W, & -b/2 \le x \le b/2 \\ 0, & \text{elsewhere.} \end{cases} \tag{B9}$$

The constant potential W can be complex to simulate the coupling to an extended system. Using the wave number $Q = \sqrt{2m^*(E - W)}$ inside the scatterer, its scattering properties are given by

$$r = \frac{P - P^{-1}}{P\rho - (P\rho)^{-1}}\, e^{-iKb} , \tag{B10}$$

$$t = \frac{\rho - \rho^{-1}}{P\rho - (P\rho)^{-1}}\, e^{-iKb} , \tag{B11}$$

where

$$\rho = \frac{K - Q}{K + Q} , \tag{B12}$$

$$P = e^{iQb} . \tag{B13}$$

ρ is the reflection coefficient of a single potential step of height W.

Since we have made the potential complex and, therefore, the Hamiltonian non-Hermitian, there will be absorption of some kind in the problem. We want our wave functions to be normalizable, that is, there should be a real k vector inside the bands. Within the band gaps, no such condition is possible so we want the wave vector to behave in the same way as in the real-potential case. Thus, in general, we require $\cos(ka)$ to be real. This implies a complex energy. For a given $\mathrm{Re}(E)$, $\cos(ka)$ is considered as a function of $\mathrm{Im}(E)$ and the condition $\mathrm{Im}[\cos(ka)] = 0$ is solved numerically. A scan of $\mathrm{Im}(E)$ will give many bands, most of which have complex k. A real k vector exists only if $\mathrm{Re}(E)$ lies inside a band.

[1] N. V. Smith and D. P. Woodruff, Prog. Surf. Sci. **21**, 295 (1986).
[2] L. C. Davis, M. P. Everson, R. C. Jaklevic, and Weidian Shen, Phys. Rev. B **43**, 3821 (1991).
[3] M. F. Crommie, C. P. Lutz, and D. M. Eigler, Nature **363**, 524 (1993).
[4] Y. Hasegawa and Ph. Avouris, Phys. Rev. Lett. **71**, 1071 (1993).
[5] D. M. Eigler and E. K. Schweizer, Nature **344**, 524 (1990).
[6] M. F. Crommie, C. P. Lutz, and D. M. Eigler, Science **262**, 218 (1993).
[7] H. Roeder, E. Hahn, H. Brune, J.-P. Bucher, and K. Kern, Nature **366**, 141 (1993).
[8] Ph. Avouris and In-Whan Lyo, Science **264**, 942 (1994).
[9] E. J. Heller, M. F. Crommie, C. P. Lutz, and D. M. Eigler, Nature **369**, 464 (1994).
[10] S. Crampin, M. H. Boon, and J. E. Inglesfield, Phys. Rev. Lett. **73**, 1015 (1994).

[11] S. Crampin, J. Phys. Condens. Matter **6**, L613 (1994).
[12] S. G. Davison and M. Steślicka, *Basic Theory of Surface States* (Oxford, New York, 1992).
[13] R. G. Newton, *Scattering Theory of Waves and Particles* (McGraw-Hill, New York, 1966).
[14] G. Hörmandinger, Surf. Sci. **296**, 1 (1993).
[15] T. C. Hsieh and T.-C. Chiang, Surf. Sci. **166**, 554 (1986).
[16] J. M. MacLaren, S. Crampin, D. D. Vvedensky, and J. B. Pendry, Phys. Rev. B **40**, 12 164 (1989); J. M. MacLaren, S. Crampin, D. D. Vvedensky, R. C. Albers, and J. B. Pendry, Comput. Phys. Commun. **60**, 365 (1990).
[17] Equations (29) and (30) hold for a steplike surface barrier. For a more realistic shape of the potential, the functions $\exp(\kappa_g^+ z)$ have to be replaced by the eigenfunctions of the barrier.
[18] A. Partridge, G. J. Tatlock, F. M. Leibsle, C. F. J. Flipse, G. Hörmandinger, and J. B. Pendry, Phys. Rev. B **48**, 8267 (1993).
[19] G. Hörmandinger, J. B. Pendry, F. M. Leibsle, P. W. Murray, R. W. Joyner, and G. Thornton, Phys. Rev. B **48**, 8356 (1993); G. Hörmandinger and J. B. Pendry, Surf. Sci. **303**, 197 (1994).
[20] V. L. Moruzzi, J. F. Janak, and A. R. Williams, *Calculated Electronic Properties of Metals* (Pergamon, New York, 1978).
[21] S. D. Kevan and R. H. Gaylord, Phys. Rev. B **36**, 5809 (1987).
[22] See, e.g., P. G. Burke, *Potential Scattering in Atomic Physics* (Plenum, New York, 1977).
[23] N. W. Ashcroft and N. D. Mermin, *Solid State Physics* (Saunders, Philadelphia, 1976).

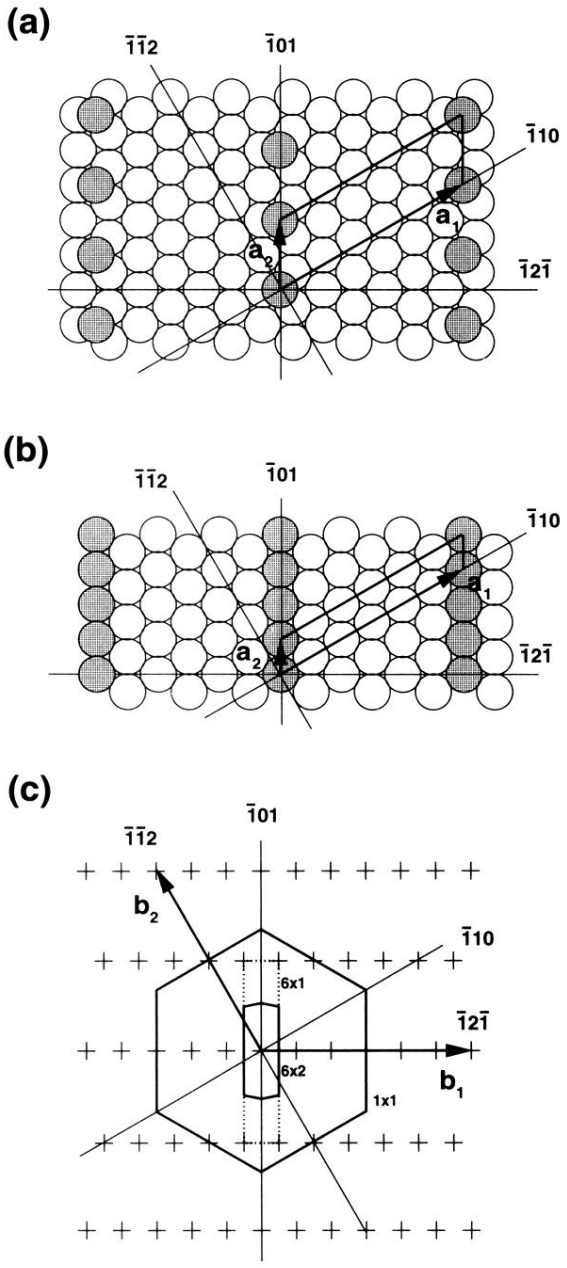

FIG. 3. (a) The geometry of the added rows used in the calculations. The unit cell is 6×2, and the unoccupied adsorption sites are filled with empty spheres (not shown). Adsorbates are indicated by shaded circles. (b) The missing-row geometry with a 6×1 unit cell. The missing atoms are replaced by empty spheres (indicated by shaded circles). (c) The Brillouin zones corresponding to (a) and (b). The large hexagon corresponds to the clean fcc (111) surface.

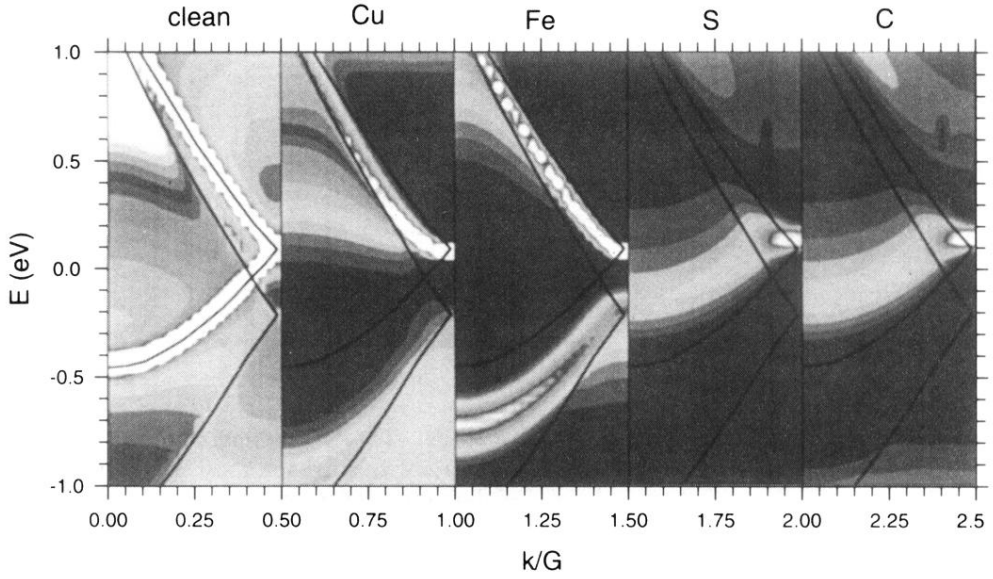

FIG. 4. The surface band structures of the Cu(111) surface with added rows along $\bar{1}01$ in a 6×2 geometry. The direction in k space is $\bar{1}2\bar{1}$ perpendicular to the rows. Contour plots of $\overline{n}(\mathbf{k}_{||}, z = 0, E)$ are shown (see text). Within each panel, $\overline{n}(\mathbf{k}_{||}, z, E)$ has been rescaled. The far left panel shows the clean Cu(111) surface, with the surface state folded back due to the sixfold supercell. In all panels, the positions of the "clean" surface state and of the bulk band edge are indicated as bold black lines. The lumpy appearance of the surface state is due to the finite grid used in the calculation. S and C show an irregularity at $\mathbf{k}_{||}/G \approx 0.4$ and $E \approx 0.6$ eV, which is due to convergence problems in the calculation of the KKR structure constants.

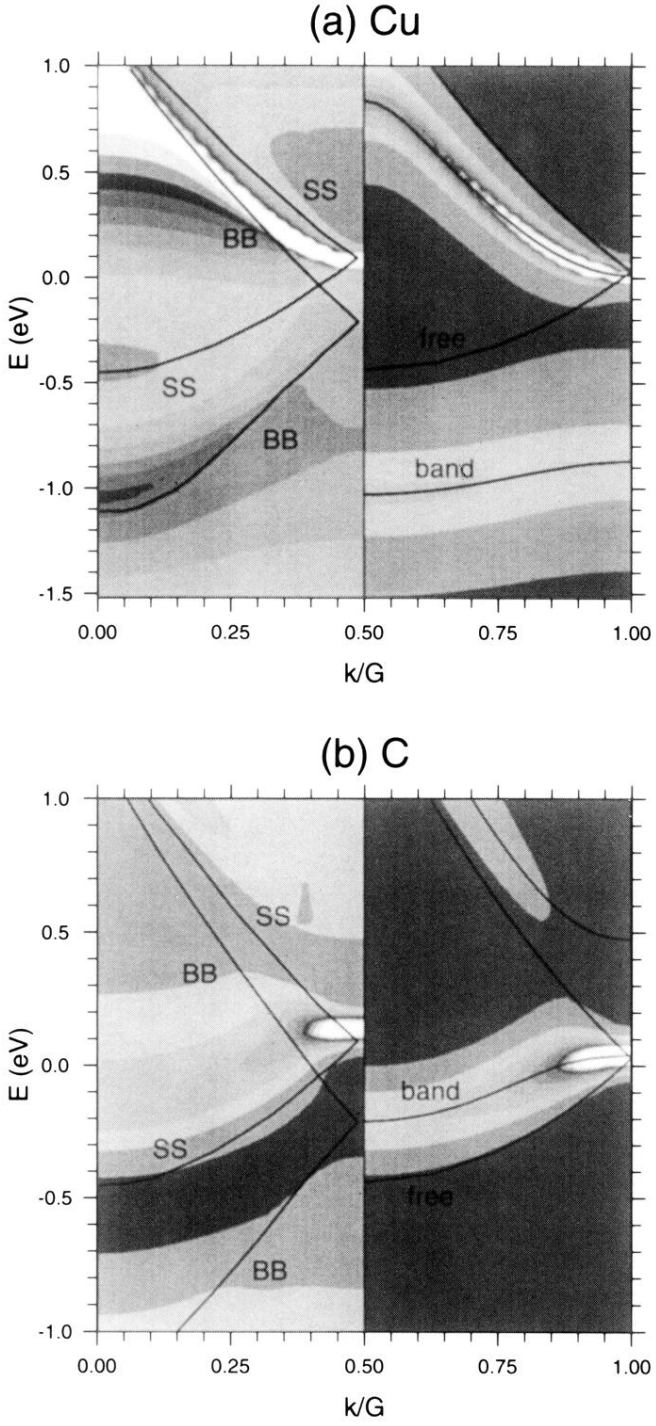

FIG. 8. The surface band structure of the Cu(111) surface with $(\bar{1}01)$ rows of adsorbates in a 6×2 geometry. The bands are shown along $\bar{1}2\bar{1}$ which is perpendicular to the rows. Contour plots of $\overline{n}(\mathbf{k}_{||}, z, E)$ are shown (see text). Left panels: the LKKR results. SS indicates the undisturbed surface state, and BB the bulk band edge. Right panels: the results of a one-dimensional model (see text). "free" indicates the free-electron band, "band" the real part of the energy eigenvalues. The contours have been generated by broadening the bands with a Lorentzian according to their imaginary parts. (a) Adsorbed Cu, (b) adsorbed C. Note that the dark structure at -1.05 eV in the Cu LKKR band structure is a maximum.